PHARMACIA

Pharmacia 70(4): 1257–1264
DOI 10.3897/pharmacia.70.e110191

Research Article

Poly (lactic-co-glycolic acid) nanoparticles for drug delivery of rupatadine fumarate: development and evaluation

Asmaa Abdelaziz Mohamed[1], Noor Zuhair Kbah[1], Osama N. Wennas[2]

1 *Department of Pharmaceutics and Pharmaceutical Industry, College of Pharmacy, Al-Zahraa University for Women, Karbala, Iraq*
2 *Department of Pharmaceutical Chemistry, College of Pharmacy, Al-Zahraa University for Women, Karbala, Iraq*

Corresponding author: Asmaa Abdelaziz Mohamed (asmaa.abdelaziz@alzahraa.edu.iq)

Received 28 July 2023 ♦ **Accepted** 17 October 2023 ♦ **Published** 1 November 2023

Citation: Mohamed AA, Kbah NZ, Wennas ON (2023) Poly (lactic-co-glycolic acid) nanoparticles for drug delivery of rupatadine fumarate: development and evaluation. Pharmacia 70(4): 1257–1264. https://doi.org/10.3897/pharmacia.70.e110191

Abstract

This study aimed to consolidate rupatadine fumarate (RF) into nanoparticles to control its release. Ten RF nanoparticles were developed by nanoprecipitation using poly (lactic-co-glycolic acid) (PLGA), polyvinyl alcohol (PVA), and Poloxamer 407 (Kolliphor P 407) in different percentages. A valid reverse-phase HPLC method was developed to assess RF in the formulated nanoparticles. The RF nanoparticles were tested chemically and morphologically. RF nanoparticles containing PLGA and PVA and Kolliphor P 407 have zeta potentials ranging from -24.4 mV±0.24 to -26.7 mV±0.05, higher than other formulations, and their release profiles were optimised. The formula (RPX3) had the best zeta potential (-26.7 mV±0.05), released about 86% of RF after 8 h and extended for 24 h. In summary, the formulation (RPX3), including 2:10:3:1.5 ratios of the drug PLGA: PVA: Kolliphor P 407 was the optimised RF-loaded nanoparticles formulation.

Keywords

controlled release, HPLC, nanoprecipitation

Introduction

Rhinitis allergies (AR) are a global health condition affecting approximately 400 million people globally. Increased urbanisation and environmental contaminants are believed to be the primary factors in AR's increasing incidence over the years. Therefore, comprehending the pathophysiology of AR is crucial to the development of innovative therapies for this illness, which usually coexist with other respiratory disorders (Muhamad et al. 2022). According to statistics, the global incidence of AR is 10–20% (Cornillier et al. 2018). RF is an antagonist of the H1 receptor that has been licensed by the European Medicines Agency (EMA), Health Canada, and Japan for AR treatment at a dose of 10 mg per tablet in patients older than 12 years. Moreover, the EMA and Health Canada have authorised RF oral solutions (Potter et al. 2016; Santamaria et al. 2021). A comparative assessment revealed that RF has the highest affinity among antihistamines and decreases platelet aggregation (Hafez et al. 2020; Church 2010). The IUPAC nomenclature for RF is 8-chloro-6, 11-dihydro-11- [1- [(5-methyl-3-pyridyl) methyl]-piperidin-4-ylidene]-5H-benzo [5,6] cyclohepta [1,2-b] pyridine fumarate (Henríquez et al. 2018), as shown in Fig. 1.

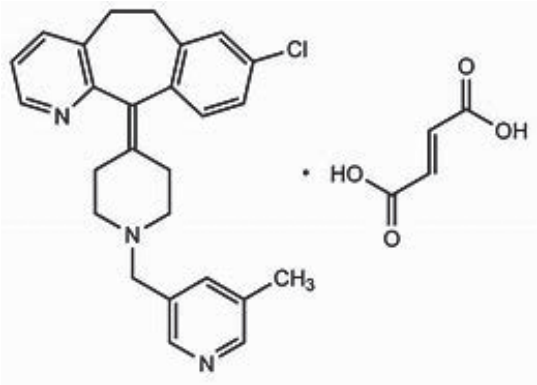

Figure 1. Chemical structure of RF.

Nanoparticles (NPs) can increase the safety and efficacy of drugs, improving stability and bioavailability (Kou et al. 2018). Polymeric NPs are becoming increasingly popular as medication delivery methods. (Karp et al. 2019). NPs can be used to control drug release (Rahi et al. 2021) by selecting a polymer with desirable chemical and molecular characteristics (Takeuchi et al. 2017), such as alginate-chitosan (Yin et al. 2021) or chitosan (Battisti et al. 2019). Furthermore, PLGA is a biodegradable polymer that can be used to prepare NPs (Zeb et al. 2022) due to their non-toxicity and easy elimination of degradation products (Elmowafy et al. 2019). PLGA has been employed to control release by regulating biodegradation (Amoyav et al. 2019; Hussain et al. 2017). Nanoparticles could provide controlled action using the appropriate polymers, such as HPMC 4000 and PLGA (Nair et al. 2019).

PLGA has numerous biomedical uses due to its biodegradability and bioavailability (Alsaab et al. 2022). The US Food and Drug Administration (FDA) has authorised the use of PLGA nanoparticles for drug delivery (Kattel et al. 2023; Ospina-Villa et al. 2019). Poloxamers, copolymers, have extensive utility in various applications as nanocarriers for hydrophobic pharmaceutical compounds (Sunoqrot et al. 2022) to enhance drug loading, stability, and solubility (Nguyen et al. 2019; Moura et al. 2020).

Although RF time to maximum plasma concentration (T_{max}) ranged from 45 min to 1 h post-oral administration, its half-life is 4.6 h (Solans et al. 2007; Shamizadeh et al. 2014). Therefore, incorporating RF into nanoparticles employing PLGA could provide a sustained profile to prolong its action, decrease plasma concentration fluctuations, and enhance the efficiency of the drug and patient compliance. In addition, PLGA polymer protects drugs from premature degradation and hepatic metabolism (Anwer et al. 2019). However, there is a lack of trials in the literature that explore the microencapsulation of RF into polymeric matrices to extend its release and achieve specific therapeutic goals. Only one study has encapsulated RF to mask the bitterness of RF through encapsulation. For instance, Wasilewska et al. (2020) conducted a study to develop oral dispersible tablets for children, aiming to mask the bitterness of RF by incorporating RF microparticles with taste-masking polymers (ethyl cellulose) using the spray drying technique. The study found that the F15 formulation, which contained Pearlitol Flash and Surelease, produced satisfactory taste masking results. Wasilewska's study produced satisfactory taste masking results, especially for the F15 formulation (which contains Pearlitol Flash and Surelease). Another study used polymers to enhance the release of RF at regular particle sizes. Roy et al. (2020) have developed and assessed oral fast-dissolving films (OFDF) of RF to enhance its release. Pullulan, hydroxypropyl methylcellulose (HPMC), and β-cyclodextrin (inclusion complex) were used in the OFDF formula, leading to a significant enhancement in the solubility of RF. Furthermore, disintegration of the drug occurred within 28 s, and the RF release was 92% after 3 h.

In our current investigation, we formulated ten RF nanoparticles by nanoprecipitation with PLGA, PVA, and Kolliphor P 407 to achieve sustained release over 24 h to overcome fluctuations in RF plasma concentration. Compatibility tests were performed to ensure the absence of undesired interactions. The microencapsulation parameters were assessed, and the nanoparticles were characterised. Moreover, the optimum nanoparticle formulation was morphologically assessed.

Materials and methods

Materials

Rupatadine fumarate (HPLC, 98.3%) and polyvinyl alcohol (Mw 90,000) were purchased from Sigma-Aldrich, USA. PLGA was purchased from Evonik Corporation, USA. Kolliphor P 407 was purchased from BASF, Germany. Methanol and acetonitrile for HPLC; E. Merck, Darmstadt, Germany. Hydrochloric acid, acetone, and sodium hydroxide pellets; Schuarlo, Spain.

Development of the HPLC method

The system components included an Agilent HPLC model HP 1260 instrument employing an Agilent 1260 photodiode array detector, a Zorbax C18 (5 µm, 25 cm × 4.6 mm) column, and 0.05 M potassium monobasic phosphate (pH 3): methanol: acetonitrile in the ratio 20:60:20 as the mobile phase. RF was assessed at 243 nm, and 50 ul was injected.

Validation of the HPLC method

The validation was performed following the ICH Harmonisation Guideline: Validation of Analytical Techniques (Q2 R1) (ICH 2005) and the United States Pharmacopoeia (USP 2020).

System suitability

Five injections of a standard solution with a concentration of 100% were used to evaluate its appropriateness. Its

properties were obtained using an HPLC apparatus (Agilent). The parameters such as theoretical plates, tailing factor, retention time, resolution, and analyte peak area were assessed and should meet the FDA's standards for acceptability (Bayoumi 2018).

Linearity

In the range of 4–20 µg/mL, we assessed RF. After constructing the standard curve, the slope, y-intercept, and coefficient (R^2) were obtained, where linearity is the capacity to acquire results directly proportional to the RF concentration, and the average area (mAu*sec) was plotted against concentrations. R2 should be greater than 0.998 as proof of an appropriate fit.

Accuracy

Accuracy indicates the closeness between anticipated and actual values. Three consecutive analyses (n = 3) were conducted in triplicate at three distinct concentrations (10.24 µg/mL, 12.8 µg/mL, and 15.36 µg/mL). The acceptable mean recovery falls within the range of 90–100%. Then, spiking using an additional percentage of RF and the accuracy of the recovered amount was determined.

Precision

We investigated repeatability and precision at the intermediate level of the HPLC method for RF using six analyses of the test concentrations. Six concentrations were measured by three separate analysers to emphasise intermediate accuracy, and the %RSD was calculated. Precision is the degree of agreement between individual tests when applied repeatedly on three separate occasions to analyse multiple replicates. The intraday precision was determined by analysing six replicates with varying RF concentrations measured on the same day. Six replicates of various RF concentrations were analysed on three separate days to determine the interday precision.

Specificity

Specificity aimed to demonstrate the ability to distinguish the principal peaks from the placebo and all related substances to confirm no interference from the excipients in the formulations.

LOD and LOQ

The lowest strength of RF that can be detected but not quantified is known as the LOD, and the lowest strength of RF that can be measured precisely enough is known as the LOQ. LOD = 3.3 × SD/S and LOQ = 10 × SD/S were employed to calculate these two parameters, where SD = standard deviation and S = slope of the standard curve.

Robustness

Robustness is the capacity to remain unaffected by slight parameter variations and to attain analysis reliability. Robustness was evaluated by analysing the impact of variations, such as wavelength and flow rate.

Stressed degradation

Base hydrolysis was done by adding 2 mL of 1M NaOH, followed by boiling for about 15 min, cooling, neutralising through the addition of 0.1 M HCl using a pH meter, and completing 100 mL with 0.1 M HCL, diluted with water, and injected into HPLC. Acid hydrolysis was performed by dissolving 5 mL of 0.5 M HCl in a conical flask, then boiling for ¼ h, cooling, and neutralising with 0.1 M NaOH using a pH meter, diluting with water, and injecting the solution into HPLC. Oxidation was performed by hydrogen peroxide after standard dissolving in 2 mL of 1 M HCL, 5 mL of 30% H2O2 solution was added, mixed, then boiled in a water bath for 15 minutes, cooling, diluting with water, and injecting the solution into HPLC.

Nanoparticles preparation

100 mg of the drug and PLGA were solubilised in 25 mL of acetone and sonicated on an ultrasonic (Elma, Germany) for 5 minutes to dissolve RF and polymer. This solution was injected into 25 mL of PVA or mixed with Kolliphor P-407 solution to make a suspension. The suspension was broken up into nanoparticles by homogenisation at 25000 rpm (GLH 850 Laboratory Homogenizer, USA), moved to a magnetic stirrer (IKA magnetic stirrer, Germany), and stirred until the organic phase completely evaporated to make a colloidal suspension of PLGA-NPs. The suspension was dried in a vacuum dryer overnight, and the nanoparticles were collected.

Table 1. Formulations for nanoparticles.

Composition*	Formulation									
	RPP1	RPP2	RPP3	RPP4	RPP5	RPX1	RPX2	RPX3	RPX4	RPX5
PLGA	0.25	0.5	0.75	1	1.5	0.25	0.5	1	1	1.5
PVA	0.1	0.2	0.3	0.4	0.5	0.1	0.2	0.3	0.4	0.5
Kolliphor P 407	–	–	–	–	–	0.05	0.1	0.15	0.2	0.3
Acetone	25	25	25	25	25	25	25	25	25	25
Water	25	25	25	25	25	25	25	25	25	25

* PLGA, PVA, and Kolliphor P 407 are in grams; acetone and water are in mL.

Characterisation of loaded nanoparticles

Zeta potential and particle size investigation

The particle size (PS), the polydispersity index (PDI), and the zeta potential (ZP) of the NPs were assessed at 25 °C employing a Zetasizer (Malvern Instruments, Malvern, UK) and dynamic light scattering (DLS) in triplicate. ZP was obtained by placing samples post-dispersion in distilled water (Oudih et al. 2023).

Estimation of drug content and entrapment efficiency

The centrifugation method was employed to calculate RF's content and entrapment efficiency. Nanoparticle powder (including RF equivalent to 10 mg) was dispersed in 5 mL acetonitrile and centrifuged at 20000 rpm for ½ h in a centrifuge (BOECO Centrifuge SC-8, Germany) to separate the supernatant. Then, the concentrated liquid was filtered, and the drug concentration was estimated. The following equations were used to determine the content and entrapment efficiency (Eltawela et al. 2021; Castro et al. 2021; Jafar et al. 2023).

$$\textit{Drug content} = \frac{\text{Actual quantity of drug loaded X 100}}{\text{Weight quantity of nanoparticles}}$$

$$\%\ \text{Entrapment efficiency} = \frac{\textbf{Weight of drug loaded in mg X 100}}{\textbf{Weight of drug initially taken in mg}}$$

Fourier transform infrared spectroscopy (FTIR)

The compatibility of RF with used polymers and its effect on their functional groups was assessed. The spectrum showed characteristic absorptions related to O-H, C=C, and C-H bonds stretching at 3491, 3050, and 2882 cm^{-1}, respectively. Moreover, the absorption band of 1705 cm^{-1} corresponds to the carbonyl groups (C=O). C=N bending at 1432 cm^{-1}, and finally, C-CL bending at 851 cm^{-1}. These findings are similar to previous literature on characteristic peaks of RF (Henríquez et al. 2018; Roy et al. 2020). The characteristic peaks are present in all spectrums of mixtures, confirming compatibility with the used polymers.

In vitro release

The release of RF from formulations that do not include Kolliphor P 407 is shown in Fig. 5. The release rate is getting slower as the amount of PVA increases. However, formulations containing Kolliphor P 407 revealed a relatively more moderate release followed by a sustained pattern (Fig. 6). The release of RF from RF-PLGA-PVA nanoparticles was less than 70% after 8 h, while most nanoparticles containing Kolliphor P 407 released ≥ 80% after 8 h. The RF nanoparticles of PLGA incorporated with PVA showed the most optimal release, especially RPX3, which released more than 86% after 8 h, then extended for twenty-four hours.

Morphology investigation

The morphology of the RF-NPs was scanned, and particle diameter and shape were assessed employing transmission electron microscopy (TEM) (Wilson et al. 2021). After appropriate dilution, a drop of the RF-NPs formulation was introduced onto a grid, and the image was examined via JEM-1400, JEOL (Tokyo, Japan).

Statistical analysis

We employ one-way analysis of variance (ANOVA) to determine the p-value of linearity.

Results and discussion

HPLC method and validation

Linearity and range

A new HPLC method was invented and validated to analyse RF, including validation parameters per ICH and USP guidance (Rahi et al. 2022). Before analysing the actual samples, the system suitability was assessed, such that the tailing factor (*T*) should not be more than 2, the capacity factor (*k'*) should be more than 2, and the plate count should not be less than 2000 (Singh et al. 2021). The parameters met the limits shown in Table 2. Fig. 2 illustrates the HPLC chromatogram of RF. Regression data confirmed good linearity, where R^2 was 0.9991, which was highly significant ($P < 0.05$). The linear regression equation was $Y = 50.737x + 33.524$, where Y represents the area (mAu*s) while x is the concentration of RF (Table 2).

Specificity

The method's high specificity was determined by analysing a placebo and a standard solution; no peak was detected near the retention time of RF, indicating its high specificity.

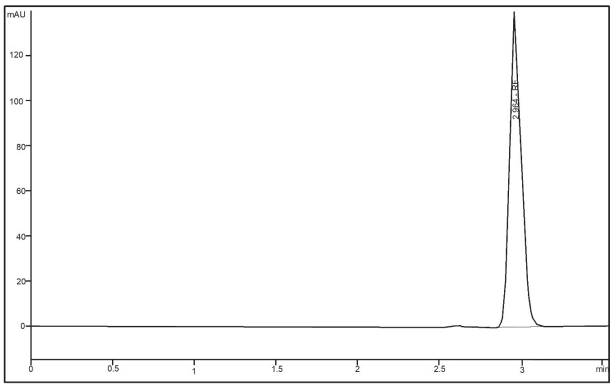

Figure 2. HPLC of RF at a retention time of 2.964 min (12.8 µg/mL of RF). Conditions: a Zorbax C18 (5 µm, 25 cm × 4.6 mm) column and 0.05 M potassium monobasic phosphate (pH 3): methanol: acetonitrile in the ratio 20:60:20 was the mobile phase. RF was detected at 243 nm.

The R^2 obtained was 0.9991 within the limits (not less than 0.99), the intercept was 33.524, and the p-value was 0.026. The method was accurate; the recovery ranged from 99.3% to 100.4%. Furthermore, the RSD values were less than 1% or complied with the limit of <2%, indicating that

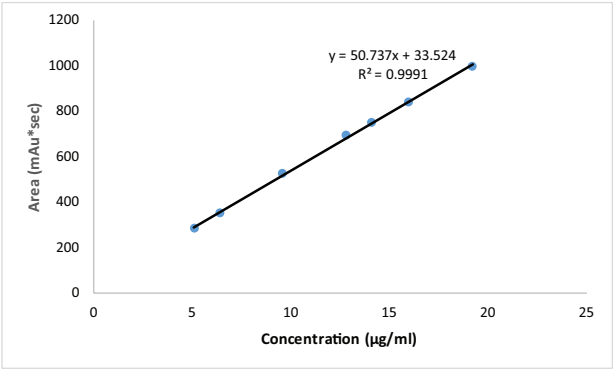

Figure 3. Calibration curve.

the method was precise based on close assessments of the same sample. The method's sensitivity was emphasised by calculating the LOD and LOQ for RF to be 2.05 µg/mL and 6.2 µg/mL, respectively. The specificity was proved by injecting a placebo, and no peaks appeared in the RF-retention time. Degradation of RF in 1M HCl, 1M NaOH, and 10% H2O2 was 7.83%, 12.09%, and 9.53%, respectively. Furthermore, the method was robust, as the RSD did not exceed 0.3% with slight variation. The results are shown in Table 2.

Table 2. Validation parameters.

	Acceptance criteria	Results
Linearity	Correlation coefficient $R^2 \geq 0.98$	0.9988
	Slope	50.831
	Intercept	32.504
	Regression equation	50.831x + 32.504
	p-value lower than 0.05	0.025
Accuracy	Mean% recovery	99.7%
	(95% to 105%)	0.36%
	RSD ≤ 2%	
Precision	Repeatability (RSD% ≤ 5%)	0.15%
	Intermediate precision (RSD% ≤ 10%)	0.31%
Sensitivity	LOD	0.667 µg/mL
	LOQ	2.022 µg/mL
Forced degradation	Recovery% in 1 M HCl	87.91% ± 0.39
	Recovery% in 1 M NaOH	92.17%± 0.11
	Recovery% in 10% H_2O_2	90.47% ± 0.25
Robustness	RSD% at a flow rate of 1.2 mL/min	0.31%
	RSD% at a flow rate of 0.8 mL/min	0.29%
	RSD% at pH 2.8	0.16%
	RSD% at pH 3.2	0.35%

*Three determinations for each n = 3

Characterization of loaded nanoparticles

Zeta potential and particle size investigation

Table 3 revealed that the mean size of RF nanoparticles ranged from 352 to 574 nm, and the zeta potential of nanoparticles comprising PLGA and PVA was in the range of -21.7±0.27 to -24.1±0.04 mV, while nanoparticles embedded in PLGA, PVA, and Kolliphor P 407 were from –24.4± 0.24 to -26.7±0.05 mV. Furthermore, the RPX3 nanoparticles prepared by PLGA, PVA, and Kolliphor P 407 matrices (1:0.3:0.15) had the highest zeta potential (-26.7 mV ± 0.05), which revealed optimum stabilisation and freedom of aggregation over time (Ibrahim et al. 2020). PDI was not uniform in nanoparticles prepared with PLGA and PVA, ranging from 0.41 to 0.62, indicating that they were highly heterogeneous, making this combination inappropriate as a drug carrier. However, particles with PLGA, PVA, and Kolliphor P 407 showed lower dispersity indices and could be considered suitable for drug delivery as their PDI ranged from 0.37 to 0.48, attributed to the uniformity of the particle size distributions (Rahi et al. 2021).

Content and entrapment efficiency

The RF content of RPP1 to RPP5 nanoparticles ranged from 57%±0.27 to 65%±0.13 and the entrapment efficiency ranged from 80.02 ±0.31 to 86.31±0.15 while RPX1 to RPX5 nanoparticles (containing Kolliphor P 407) content uniformity and entrapment were 67.3±0.17 to 71.9 ±0.24 and 79.56 ± 0.12 to 89.14±0.16, respectively, as shown in Table 3.

Fourier transform infrared spectroscopy (FTIR)

The compatibility of RF with used polymers and its effect on their functional groups was assessed. The spectrum showed characteristic absorptions related to O-H, C=C, and C-H bonds stretching at 3491, 3050, and 2882 cm-1, respectively. Moreover, the absorption band of 1705 cm-1 corresponds to the carbonyl groups (C=O). C=N bending at 1432 cm-1, and finally, C-CL bending at 851 cm-1. These findings are similar to previous literature on characteristic peaks of RF (Henríquez et al. 2018; Roy et al. 2020). The characteristic peaks are present in all spectrums of mixtures, confirming compatibility with the used polymers.

Table 3. Characteristics of RF Nanoparticles.

Formula	Drug Content* (%) ± SD	Efficiency entrapment (%) ± SD	Zeta Potential* (mV) ± SD	Mean particle size* (nm) ± SD	PDI*
RPP1	61±0.21	86.31±0.15	-21.9±0.09	388.0 ±1.7	0.41±0.01
RPP2	65±0.13	80.02±0.31	-23.8±0.19	457.2±1.6	0.54±0.02
RPP3	63±0.11	81.00±0.26	-22.2±0.07	547.1±1.3	0.62±0.01
RPP4	59±0.31	85.78±0.30	-24.1±0.05	467.2±1.8	0.49±0.02
RPP5	57±0.27	83.14±0.32	-21.7±0.27	428.0±0.9	0.48±0.01
RPX1	67±0.28	88.12±0.13	-25.3±0.13	352.0±1.1	0.48±0.02
RPX2	68±0.14	85.19±0.12	-24.4±0.24	447.3±1.3	0.42±0.01
RPX3	69±0.18	89.14±0.16	-26.7±0.05	415.0±2.4	0.37±0.01
RPX4	67.3±0.17	81.7±0.24	-26.1±0.11	379.4±1.2	0.37±0.02
RPX5	71.9±0.24	79.56±0.19	-25.1±0.02	574.3±1.1	0.47±0.01

*Values are stated as mean ± SD, n = 3.

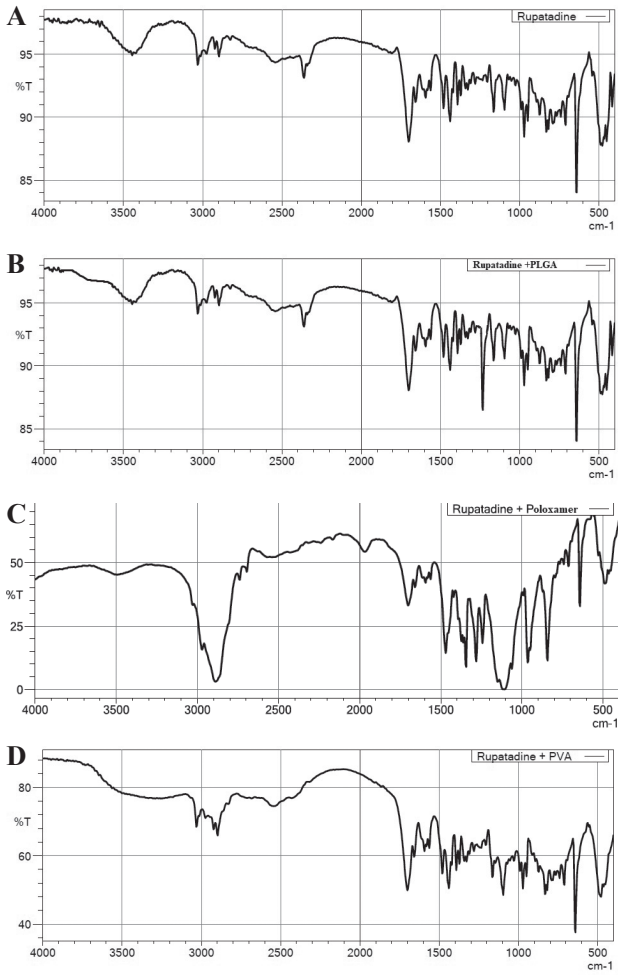

Figure 4. The FT-IR spectra of **A** RF **B** RF+ PLGA **C** RF+ poloxamer 407 (Kolliphor P 407), and **D** RF+PVA.

In vitro release

The release of RF from formulations that do not include Kolliphor P 407 is shown in Fig. 5. The release rate is getting slower as the amount of PVA increases. However, formulations containing Kolliphor P 407 revealed a relatively more moderate release followed by a sustained pattern (Fig. 6). The release of RF from RF-PLGA-PVA nanoparticles was less than 70% after 8 h, while most nanoparticles containing Kolliphor P 407 released ≥ 80% after 8 h. The RF nanoparticles of PLGA incorporated with PVA showed the most optimal release, especially RPX3, which released more than 86% after 8 h, then extended for twenty-four hours.

Morphology investigation

Based on the results mentioned, the formulation RPX3 was chosen for more research because the nanoparticles were about 415 nm in size, the zeta potential was -26.7 mV, and the best release was 86% after 8 hours. Fig. 7 revealed the TEM photograph of RF nanoparticles (RPX3), where the nanoparticles had a uniform surface and a spherical shape and did not aggregate.

Many researchers used PLGA to modify the release of some drugs. For instance, Patra et al. (2022) formulated

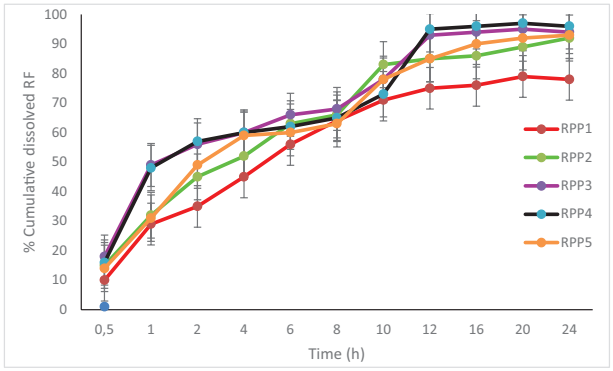

Figure 5. Release of RF nanoparticles (values represent mean ±SD, n = 6).

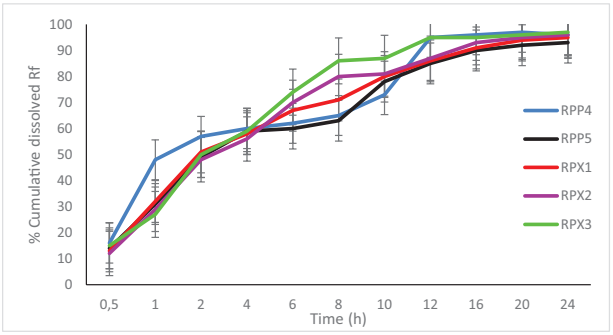

Figure 6. Release of RF nanoparticles (values represent mean ±SD, n = 6).

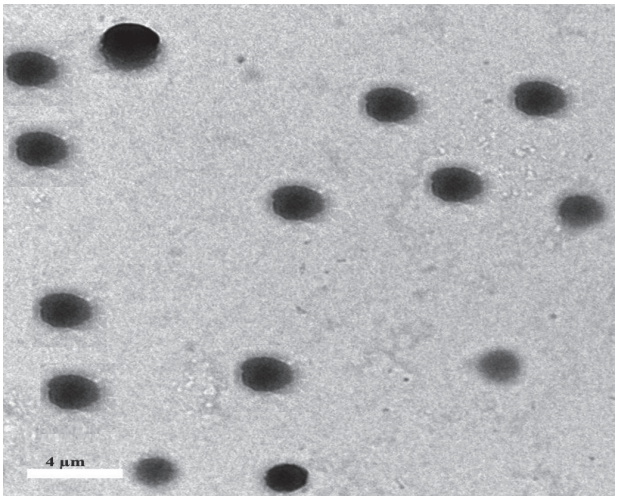

Figure 7. TEM photograph of the selected formula (RPX3) nanoparticles (scale bar).

nanoparticles of genistein (GA) using PLGA and polyethylene glycol (PEG). They found that PLGA-PEG-GA nanoparticles were better than nanoparticles that did not contain PEG. Furthermore, in our current work, we formulated PLGA-loaded extended-release RF nanoparticles, the first trial to microencapsulate RF using PLGA into controlled-release nanoparticles with enhanced characteristics such as high drug content, excellent entrapment, efficiency, and prolonged release. Among the ten prepared

formulations, the release of RF from RPX3 was more than 85% after 8 h and maintained an almost sustainable level for 24 h. Therefore, the optimum formulation was RPX3, which showed the best characteristics.

Conclusion

The incorporation of RF into nanoparticles employing PLGA, PVA, and Kolliphor P 407 through nanoprecipitation resulted in enhanced characteristics, including optimal production yield, high drug content, exceptional drug entrapment efficiency, and sustained release to avoid fluctuation in RF plasma concentration. Therefore, NPs containing PLGA, PVA, and Kolliphor P 407 can be alternatives to the current conventional dosage forms for the delivery of RF with improved properties and bioavailability.

Acknowledgement

The authors appreciate Al-Zahraa University for women support.

References

Alsaab HO, Alharbi FD, Alhibs AS, Alanazi NB, Alshehri BY, Saleh MA, Alshehri FS, Algarni MA, Almugaiteeb T, Uddin MN, Alzhrani R (2022) PLGA-based nanomedicine: History of advancement and development in clinical applications of multiple diseases. Pharmaceutics 14: e2728. https://doi.org/10.3390/pharmaceutics14122728

Amoyav B, Benny O, Amoyav B, Benny O (2019) Microfluidic based fabrication and characterization of highly porous polymeric microspheres. Polymers 11(3): e419. https://doi.org/10.3390/polym11030419

Anwer MK, Mohammad M, Ezzeldin E, Fatima F, Alalaiwe A, Iqbal M (2019) Preparation of sustained release apremilast-loaded PLGA nanoparticles: in vitro characterization and in vivo pharmacokinetic study in rats. International Journal of Nanomedicine 14: 1587–1595. https://doi.org/10.2147/IJN.S195048

Battisti M, Vecchione R, Casale C, Pennacchio FA, Lettera V, Jamaledin R, Profeta M, Di Natale C, Imparato G, Urciuolo F, Netti P (2019) Non-invasive production of multi-compartmental biodegradable polymer microneedles for controlled intradermal drug release of labile molecules. Frontiers in Bioengineering and Biotechnology 7: e296. https://doi.org/10.3389/fbioe.2019.00296

Bayoumi A (2018) Formulation, optimization, and evaluation of sitagliptin and simvastatin rapidly dissolving tablets. International Journal of Applied Pharmaceutics 10: e270. https://doi.org/10.22159/ijap.2018v10i5.28122

Castro SR, Ribeiro LNM, Breitkreitz MC, Guilherme VA, Rodrigues SGH, Mitsutake H, Alcântara ACS, Yokaichiya F, Franco MKKD, Clemens D, Kent B, Lancellotti M, de Araújo DR, de Paula E (2021) A pre-formulation study of tetracaine loaded in optimized nanostructured lipid carriers. Scientific Reports 11: e21463. https://doi.org/10.1038/s41598-021-99743-6

Cornillier H, Giraudeau B, Munck S, Hacard F, Jonville-Bera A-P, d'Acremont G, Pham B-N, Maruani A (2018) Chronic spontaneous urticaria in children – a systematic review on interventions and comorbidities. Pediatric Allergy and Immunology 29(3): 303–310. https://doi.org/10.1111/pai.12870

Church M (2010) Efficacy and tolerability of rupatadine at four times the recommended dose against histamine- and platelet-activating factor-induced flare responses and ex vivo platelet aggregation in healthy males. The British Journal of Dermatology 163: 1330–1332. https://doi.org/10.1111/j.1365-2133.2010.10029.x

Elmowafy EM, Tiboni M, Soliman ME (2019) Biocompatibility, biodegradation and biomedical applications of poly(lactic acid)/poly(lactic-co-glycolic acid) micro and nanoparticles. Journal of Pharmaceutical Investigation 49: 347–380. https://doi.org/10.1007/s40005-019-00439-x

Eltawela S, Abdelaziz E, Mahmoud M, Elghamry H (2021) Preparation and characterization of (−)-epigallocatechin gallate lipid based nanoparticles for enhancing availability and physical properties. Al-Azhar Journal of Pharmaceutical Sciences 63(1): 17–36. https://doi.org/10.21608/ajps.2021.153558

Hafez HM, Abdel-Hakeem EA, Hassanein H (2020) Rupatadine, a dual antagonist of histamine and platelet-activating factor (PAF), attenuates experimentally induced diabetic nephropathy in rats. Naunyn-Schmiedeberg's Archives of Pharmacology 393(8): 1487–1500. https://doi.org/10.1007/s00210-020-01856-8

Henríquez L, Madrigal Redondo G, Vargas Zuñiga R, Carazo G (2018) Identification of rupatadine fumarate polymorphic crystalline forms in pharmaceutical raw materials.

Hussain M, Xie J, Hou Z, Shezad K, Xu J, Wang K, Gao Y, Shen L, Zhu J (2017) Regulation of drug release by tuning surface textures of biodegradable polymer microparticles. ACS Applied Materials & Interfaces 9(16): 14391–14400. https://doi.org/10.1021/acsami.7b02002

Ibrahim HM, Awad M, Al-Farraj AS, Al-Turki AM (2020) Stability and Dynamic Aggregation of Bare and Stabilized Zero-Valent Iron Nanoparticles under Variable Solution Chemistry. Nanomaterials 10(2): e192. https://doi.org/10.3390/nano10020192

ICH (2005) Validation of Analytical Procedures: Text and Methodology. International Conference on Harmonization (ICH), Q2(R1), Geneva, 17 pp.

Jafar M, Khan M, Salahuddin M, Zahoor S, Slais H, Alalwan L, Alshaban H (2023) Development of apigenin loaded gastroretentive microsponge for the targeting of *Helicobacter pylori*. Saudi Pharmaceutical Journal 31(5): 659–668. https://doi.org/10.1016/j.jsps.2023.03.006

Karp F, Busatto C, Turino L, Luna J, Estenoz D (2019) PLGA nano-and microparticles for the controlled release of florfenicol: experimental and theoretical study. Journal of Applied Polymer Science 136(12): e47248. https://doi.org/10.1002/app.47248

Kattel P, Sulthana S, Trousil J, Shrestha D, Pearson D, Aryal S (2023) Effect of nanoparticle weight on the cellular uptake and drug delivery potential of PLGA nanoparticles. ACS Omega 8(30): 27146–27155. https://doi.org/10.1021/acsomega.3c02273

Kou L, Bhutia Y, Yao Q, He Z, Sun J, Ganapathy V (2018) Transporter-guided delivery of nanoparticles to improve drug permeation across cellular barriers and drug exposure to selective cell types. Frontiers in Pharmacology 9: 1–16. https://doi.org/10.3389/fphar.2018.00027

Moura S, Noro J, Cerqueira P, Silva C, Cavaco-Paulo A, Loureiro A (2020) Poloxamer 407 based-nanoparticles for controlled release of methotrexate. International Journal of Pharmaceutics 575: e118924. https://doi.org/10.1016/j.ijpharm.2019.118924

Muhamad H, Tan H, Shukri N, Mohd Ashari N, Wong K (2022) Allergic Rhinitis: A Clinical and Pathophysiological Overview. Frontiers in Medicine 9: 874114. https://doi.org/10.3389/fmed.2022.874114

Nair AB, Sreeharsha N, Al-Dhubiab BE, Hiremath JG, Shinu P, Attimarad M, Venugopala KN, Mutahar M (2019) HPMC- and PLGA-based nanoparticles for the mucoadhesive delivery of sitagliptin: Optimization and in vivo evaluation in rats. Materials 12(24): e4239. https://doi.org/10.3390/ma12244239

Nguyen VT, Nguyen TH, Dang LH, Vu-Quang H, Tran NQ (2019) Folate-conjugated chitosan-pluronic P123 nanogels: Synthesis and characterizations towards dual drug delivery. Journal of Nanomaterials 2019: 1–14. https://doi.org/10.1155/2019/1067821

Ospina-Villa JD, Gómez-Hoyos C, Zuluaga-Gallego R, Triana-Chávez O (2019) Encapsulation of proteins from *Leishmania panamensis* into PLGA particles by a single emulsion-solvent evaporation method. Journal of Microbiological Methods 162: 1–7. https://doi.org/10.1016/j.mimet.2019.05.004

Oudih B, Tahtat D, Khodja A, Mahlous M, Hammache Y, Guittoum A, Kebbouche-Gana S (2023) Chitosan nanoparticles with controlled size and zeta potential. Polymer Engineering & Science 63(8): 1–11. https://doi.org/10.1002/pen.26261

Patra A, Satpathy S, Naik P, Kazi M, Hussain M (2022) Folate receptor-targeted PLGA-PEG nanoparticles for enhancing the activity of genistein in ovarian cancer. Artificial Cells, Nanomedicine, and Biotechnology 50: 228–239. https://doi.org/10.1080/21691401.2022.2118758

Potter P, Mitha E, Barkai L, Mezei G, Santamaria E, Izquierdo I, Maurer M (2015) Rupatadine is effective in the treatment of chronic spontaneous urticaria in children aged 2–11 years. Pediatric Allergy and Immunology 27(1): 55–61. https://doi.org/10.1111/pai.12460

Rahi F, Sheet M, Fayyadh MS (2021) Linagliptin and gliclazide di-loaded extended-release nanoparticles: formulation and evaluation. Wiadomości Lekarskie 74(9 cz 2): 2315–2322. https://doi.org/10.36740/WLek202109212

Rahi F, Sheet M, Jawad K (2022) Preparation and evaluation of lipid matrix microencapsulation for drug delivery of azilsartan kamedoxomil. ScienceRise: Pharmaceutical Science 2022: 21–28. https://doi.org/10.15587/2519-4852.2022.270306

Roy A, Arees R, Blr M (2020) Formulation development of oral fast-dissolving films of rupatadine fumarate. Asian Journal of Pharmaceutical and Clinical Research: 67–72. https://doi.org/10.22159/ajpcr.2020.v13i11.39185

Santamaria E, Izquierdo I, Valle M (2021) Rupatadine oral solution titration by body weight in paediatric patients suffering from allergic rhinitis: A Population pharmacokinetic study. The Journal of Clinical Pharmacology 13: 115–122. https://doi.org/10.2147/CPAA.S312911

Singh N, Akhtar MJ, Anchliya A (2021) Development and validation of HPLC method for simultaneous estimation of reduced and oxidized glutathione in bulk pharmaceutical formulation. Austin Journal of Analytical and Pharmaceutical Chemistry 8(1): e1129. https://doi.org/10.26420/austininternmed.2021.1129

Shamizadeh S, Brockow K, Ring J (2014) Rupatadine: efficacy and safety of a non-sedating antihistamine with PAF-antagonist effects. Allergo Journal International 23(3): 87–95. https://doi.org/10.1007/s40629-014-0011-7

Solans A, Banús M, Juana P, Nadal T, Izquierdo I, Merlos M (2007) Influence of food on the oral bioavailability of rupatadine tablets in healthy volunteers: A single-dose, randomized, open-label, two-way crossover study. Clinical Therapeutics 29: 900–908. https://doi.org/10.1016/j.clinthera.2007.05.004

Sunoqrot S, Aliyeh S, Abusulieh S, Sabbah D (2022) Vitamin E TPGS-poloxamer nanoparticles entrapping a novel PI3Kα inhibitor potentiate its activity against breast cancer cell lines. Pharmaceutics 14: e1977. https://doi.org/10.3390/pharmaceutics14091977

Takeuchi I, Tomoda K, Hamano A, Makino K (2017) Effects of physicochemical properties of poly(lactide-*co*-glycolide) on drug release behavior of hydrophobic drug-loaded nanoparticles. Colloids and Surfaces A 520: 771–778. https://doi.org/10.1016/j.colsurfa.2017.02.054

USP [The Pharmacopoeia of United States of America] (2020) The Pharmacopoeia of United States of America (43th edn.). National Formulary 38, Mack Publishing Co. Easton, vol. 2, Electronic version.

Wasilewska K, Ciosek-Skibińska P, Lenik J, Srčič S, Basa A, Winnicka K (2020) Utilization of ethylcellulose microparticles with rupatadine fumarate in designing orodispersible minitablets with taste masking effect. Materials 13(12): e2715. https://doi.org/10.3390/ma13122715

Wilson BK, Prud'homme RK (2021) Nanoparticle size distribution quantification from transmission electron microscopy (TEM) of ruthenium tetroxide stained polymeric nanoparticles. Journal of Colloid and Interface Science 604: 208–220. https://doi.org/10.1016/j.jcis.2021.04.081

Yin XB, Yu QZ, Li BW, Zhang CD (2021) Preparation and characterization of sodium alginate/chitosan composite nanoparticles loaded with chondroitin sulfate. Advances in Materials Science and Engineering 2021: e6665488. https://doi.org/10.1155/2021/6665488

Zeb A, Gul M, Nguyen TTL, Maeng H (2022) Controlled release and targeted drug delivery with poly(lactic-co-glycolic acid) nanoparticles: reviewing two decades of research. Journal of Pharmaceutical Investigation 52: 683–724. https://doi.org/10.1007/s40005-022-00584-w